Supporting Information

A wash-free AIE fluorescent probe for monitoring lipid droplets and identifying tumor

Xue Zhang[a,b], Jie Wang[a,b], Sichen Zhang[a,b], Jiale Li[a,b], Aobo Sun[a,b], Tianjian Wei[a], Chunfei Wang[a,b,], Lei Hu[a,b,*], Lutan Zhou[a,b,*], Hui Wang[a,b,*]

[a] Anhui Innovative Center for Drug Basic Research of Metabolic Diseases, Wannan Medical College, Wuhu 241002, China

[b] School of Pharmacy, Wannan Medical College, Wuhu 241002, China

* Corresponding author

E-mail address: hulei@wnmc.edu.cn (Lei Hu); zhoulutan2021@163.com (Lutan Zhou); wanghias@126.com (Hui Wang)

Experimental section

Materials and instruments: Unless otherwise specified, all reagents were purchased from Shanghai Aladdin Reagents Ltd. LTD. The UV-visible absorption spectra of all compounds in different solvents were tested using a UV-5900 PC UV-visible spectrometer. The fluorescence emission spectra of all compounds were recorded with a Hitachi F-4600 fluorescence spectrophotometer at room temperature. Biological imaging of the cells was performed using a Leica TCS SP8 confocal laser scanning microscope.

Synthesis

TCO1: Weigh the appropriate amounts of compounds M1 and M2 in a 100 mL round-bottom flask. Compounds M1 and M2 were reacted in a molar ratio of 1:1.2 (M1: 0.35 g; M2: 0.12 g), using ethanol as the solvent and adding 50 μL of piperidine as the catalyst. The reaction was refluxed for four days. After completion of the reaction, the solution containing compound **TCO1** was filtered while hot, eluted with ethanol two to three times, and then dried to yield a deep red solid weighing 0.15 g. The percentage yield of compound **TCO1** is about 29.2%. ^{1}H NMR (400 MHz, d_6-DMSO) δ 8.55 (s,

1H), 7.72 (d, *J* = 8.8 Hz, 1H), 7.64 (d, *J* = 15.5 Hz, 1H), 7.59-7.50 (m, 3H), 7.47 (t, *J* = 7.8 Hz, 4H), 7.32-7.28 (m, 6H), 6.77-6.67 (m, 3H), 6.50 (d, *J* = 1.9 Hz, 1H), 3.43-3.38 (m, 4H), 1.12 (t, *J* = 7.0 Hz, 6H). ^{13}C NMR (126 MHz, $CDCl_3$) δ 185.90, 160.18, 157.20, 153.43, 149.80, 147.38, 145.48, 145.44, 131.26, 130.62, 129.92, 126.71, 125.91, 122.40, 120.81, 118.73, 116.12, 112.08, 111.28, 104.81, 44.52, 12.62. HRMS: calculated 514.2256; found 515.2347 ($[M+H]^+$).

TCO2: Weigh the appropriate amounts of M1 and M2 into a 100 mL round-bottom flask. The compounds M1 and M2 were reacted in a molar ratio of 1:1.2 (M1: 0.35 g; M3: 0.14 g), using ethanol as the solvent and adding 50 μL of piperidine as the catalyst. The reaction was refluxed for four days. After cooling the reaction system to room temperature, vacuum suction filtration was performed, followed by spin-drying of the filtrate and purification through column chromatography. The eluate from column chromatography consisted of petroleum ether and ethyl acetate, with a final volume ratio of petroleum ether to ethyl acetate being 10:1. This process yielded a deep red product weighing 0.04 g. The percentage yield of compound **TCO2** is about 7.0%. ^{1}H NMR (400 MHz, d_6-DMSO) δ 8.55 (s, 1H), 7.71 (t, *J* = 9.0 Hz, 1H), 7.64 (d, *J* = 15.4 Hz, 1H), 7.57-7.43 (m, 6H), 7.36-7.25 (m, 7H), 6.81 – 6.63 (m, 3H), 6.50 (d, J = 2.1 Hz, 1H), 3.42-3.37 (m, 4H), 1.56-1.48 (m, 4H), 1.35-1.29 (m, 4H), 0.92 (t, J = 7.3 Hz,6H). ^{13}C NMR (126 MHz, $CDCl_3$) δ 185.99, 160.03, 157.26, 153.31, 147.51, 145.46, 131.18, 130.63, 129.94, 129.81, 129.34, 127.10, 126.72, 125.93, 124.44, 116.13, 111.81, 110.77, 104.85, 50.94, 34.54, 29.70, 20.30, 13.93. HRMS: calculated 570.2882; found 571.2957 ($[M+H]^+$).

TCN1: Weigh the appropriate amounts of compounds M4 and M5 in a 100 mL round-bottom flask. Compounds M4 and M5 were reacted in a molar ratio of 1:1.1 (M4: 0.08 g; M5: 0.04 g) using ethanol as the solvent, with the addition of 50 μL of piperidine as a catalyst. The condensation reaction for compound **TCN1** was carried out for 12 hours at a temperature of 80°C. For purification, column chromatography was

performed using an eluent composed of petroleum ether and ethyl acetate in a volume ratio of 30:1. Ultimately, a deep red solid weighing 0.04 g was obtained as the final product. The percentage yield of compound **TCN1** is about 7.1%. ^{1}H NMR (400 MHz, d_6-DMSO) δ 8.15 (s, 1H), 7.63-7.58 (m, 3H), 7.51-7.38 (m, 5H), 7.34-7.24 (m, 6H), 7.19-7.12 (m, 1H), 6.82 (dd, J = 8.7, 2.3 Hz, 1H), 6.75 (d, J = 9.1 Hz, 2H), 6.61 (d, J = 2.2 Hz, 1H), 3.48-3.43 (m, 4H), 1.13 (t, J = 7.0 Hz, 6H). ^{13}C NMR (126 MHz, $CDCl_3$) δ 164.59, 158.18, 156.20, 152.80, 145.52, 144.40, 131.83, 129.95, 129.35, 126.55, 125.85, 124.37, 116.47, 110.72, 105.74, 34.98, 31.92, 31.50, 31.43, 30.33, 30.15, 29.69, 29.35, 22.68, 14.09, 12.37. HRMS: calculated 562.2369; found 563.2459 ($[M+H]^+$).

TCN2: Weigh the appropriate amounts of M4 and M6 in a 100 mL round-bottom flask. The reaction between M4 and M6 was conducted in a 1:2 molar ratio (M4: 0.2 g; M6: 0.23 g) using ethanol as the solvent, with the addition of 50 μL of piperidine as a catalyst. The mixture was heated and condensed at 80°C for 15 hours. Next, filter the solution to remove yellow solid impurities, followed by column chromatography. The eluent used is a mixture of petroleum ether and ethyl acetate in a volume ratio of 20:1 (v/v). Finally, purification was carried out using silica gel plates, resulting in the isolation of 0.2 g of deep-red solid product. The percentage yield of compound **TCN2** is about 32.3%. ^{1}H NMR (400 MHz, d_6-DMSO) δ 8.14 (s, 1H), 7.63-7.56 (m, 3H), 7.51-7.40 (m, 5H), 7.31-7.25 (m, 6H), 7.19-7.10 (m, 1H), 6.81 (dd, J = 8.7, 2.3 Hz, 1H), 6.73 (d, J = 9.1 Hz, 2H), 6.61 (d, J = 2.2 Hz, 1H), 3.40-3.35 (m, 4H), 1.57-1.47 (m, 4H), 1.37-1.31 (m, 4H), 0.91 (t, J = 7.3 Hz, 6H). ^{13}C NMR (126 MHz, $CDCl_3$) δ 164.82, 158.34, 156.41, 153.03, 145.55, 144.66, 131.81, 129.96, 129.35, 126.57, 125.85, 116.49, 111.17, 105.77, 29.70, 29.25, 20.24, 13.87. HRMS: calculated 618.2995; found 619.3074 ($[M+H]^+$).

Oil/water partition coefficients measurement

The $logP_{o/w}$ values for all probes were determined using a shake-flask method. A 10 μM solution of each probe was prepared and partitioned in a mixture of octanol (5

mL) and water (5 mL). The mixture was vortexed thoroughly and then centrifuged at 5000 rpm for 5 minutes to facilitate phase separation. The absorbance of the resulting octanol and water layers was measured using UV-vis spectroscopy. The logP value was calculated using the following equation: logP =log(Ao/Aw),where Ao and Aw represent the absorbance of the probes in octanol and water, respectively.

MTT assays

HepG2 cells were plated into individual wells of a 96-well plate at a density of 10^5 cells/well for conducting cell viability experiments. The cells were cultured until they reached approximately 85% confluence prior to treatment initiation within these plates. Triplicate wells received treatments with **TCO1**, **TCO2**, **TCN1** and **TCN2** at specified concentrations. Prior to administering these compounds, fresh cell culture media replaced existing media while aliquots from stock solutions underwent dilution steps necessary for achieving desired final concentrations. Following an incubation period lasting 24 hours, fresh DMEM medium supplemented each well by replacing previous media content entirely. Subsequently, MTT solution (5 mg/mL) was added to each well (10 μL/well) and incubated for an additional 4 hours at 37°C with 5% CO_2. Following removal of the MTT medium, formazan crystals were dissolved in DMSO (100 μL/well), and absorbance was measured at a wavelength of 590 nm using a microplate reader (Infinite2000pro).

Cell imaging

HepG2 cells were seeded in 35 mm glass bottom plates at a density of 1×10^5 cells. Prior to treatment, the cells were grown to approximately 65% confluence in the plates. **TCO1, TCO2, TCN1** and **TCN2** were initially dissolved in DMSO to obtain a stock solution with a concentration of 1 mM, which was then diluted with DMEM cell culture medium to achieve the working concentration of 10 μM. For live cell imaging, the cells were incubated with **TCO1, TCO2, TCN1** and **TCN2** (10 μM) in cell medium containing 10% FBS and maintained at a temperature of 37 °C in an atmosphere consisting of 5% CO_2 and 95% air for a duration of 30 minutes. Subsequently, the cells

were washed either with or without PBS buffer prior to imaging. The cellular imaging process was conducted using a Leica TCS SP8 confocal laser scanning microscope, while image data acquisition and processing were performed utilizing Image J. For **TCO1**, λ_{ex}=442 nm, λ_{em}= 550-620 nm. For **TCO2**, λ_{ex}=442 nm, λ_{em}= 550-620 nm. For **TCN1**, λ_{ex}=514 nm, λ_{em}= 560-650 nm. For **TCN2**, λ_{ex}=514 nm, λ_{em}= 560-650 nm.

Co-localization experiments

Co-staining was performed using 1 μM BODIPY 493/503 for 30 min. For BODIPY, λ_{ex}= 488 nm; λ_{em}= 490-540 nm. For **TCO1**, λ_{ex}=442 nm, λ_{em}= 550-620 nm.

Animal model and organ imaging

We have exerted ourselves to reduce the number of animals used in these studies and also taken effort to reduce animal suffering from pain and discomfort. We utilized the 4T1 cell (mouse breast cancer cells) BALB/c mouse model by feeding normal forage. The mice in the experiment developed a tumor of appropriate size in their legs after ten days. Compound **TCO1** was administered via injection into the tumor site of the mice, and after a duration of 3 hours, the mice were euthanized for organ dissection and subsequent imaging (including heart, liver, spleen, lung, kidney and tumors). The organ images were then acquired using a Perkin Elmer IVIS Lumina LT series III mouse living image system.

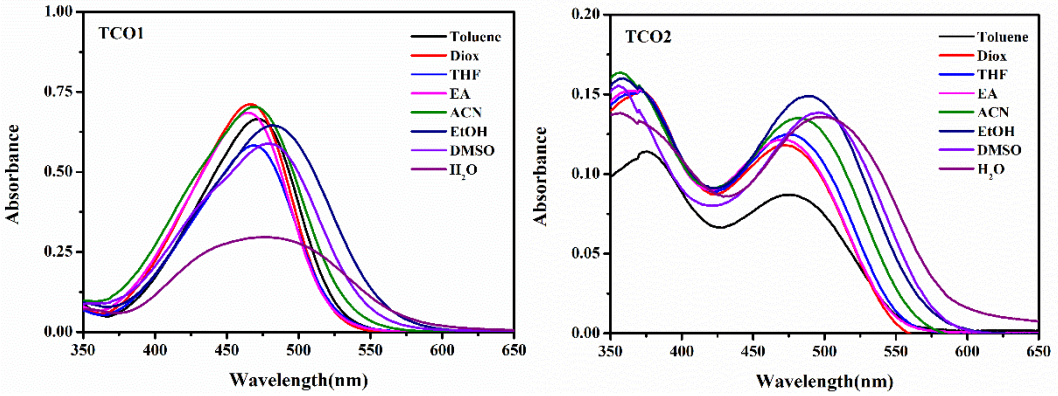

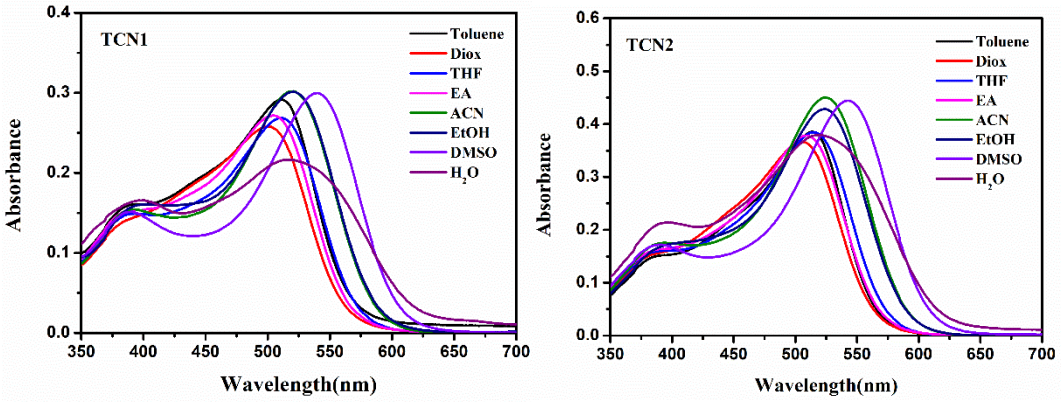

Fig. S1 The absorption spectra of compounds **TCO1**, **TCO2**, **TCN1** and **TCN2** in different solvents.

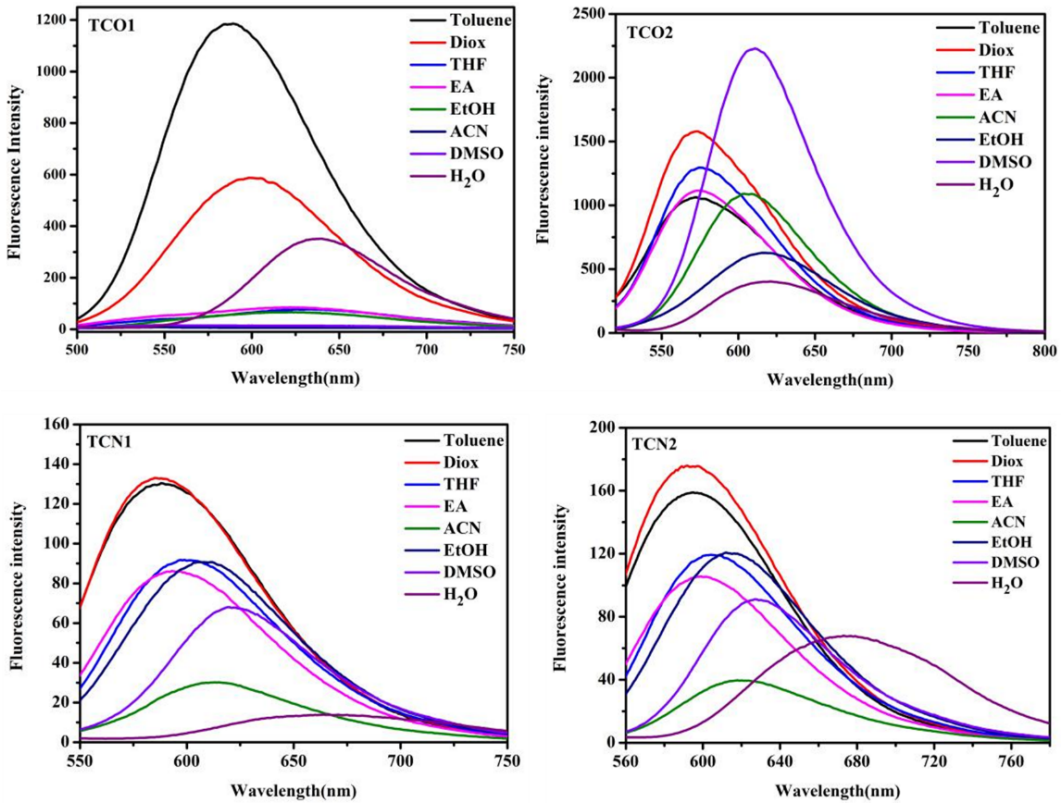

Fig. S2 Fluorescence intensity of compounds **TCO1**, **TCO2**, **TCN1** and **TCN2** in different solvents.

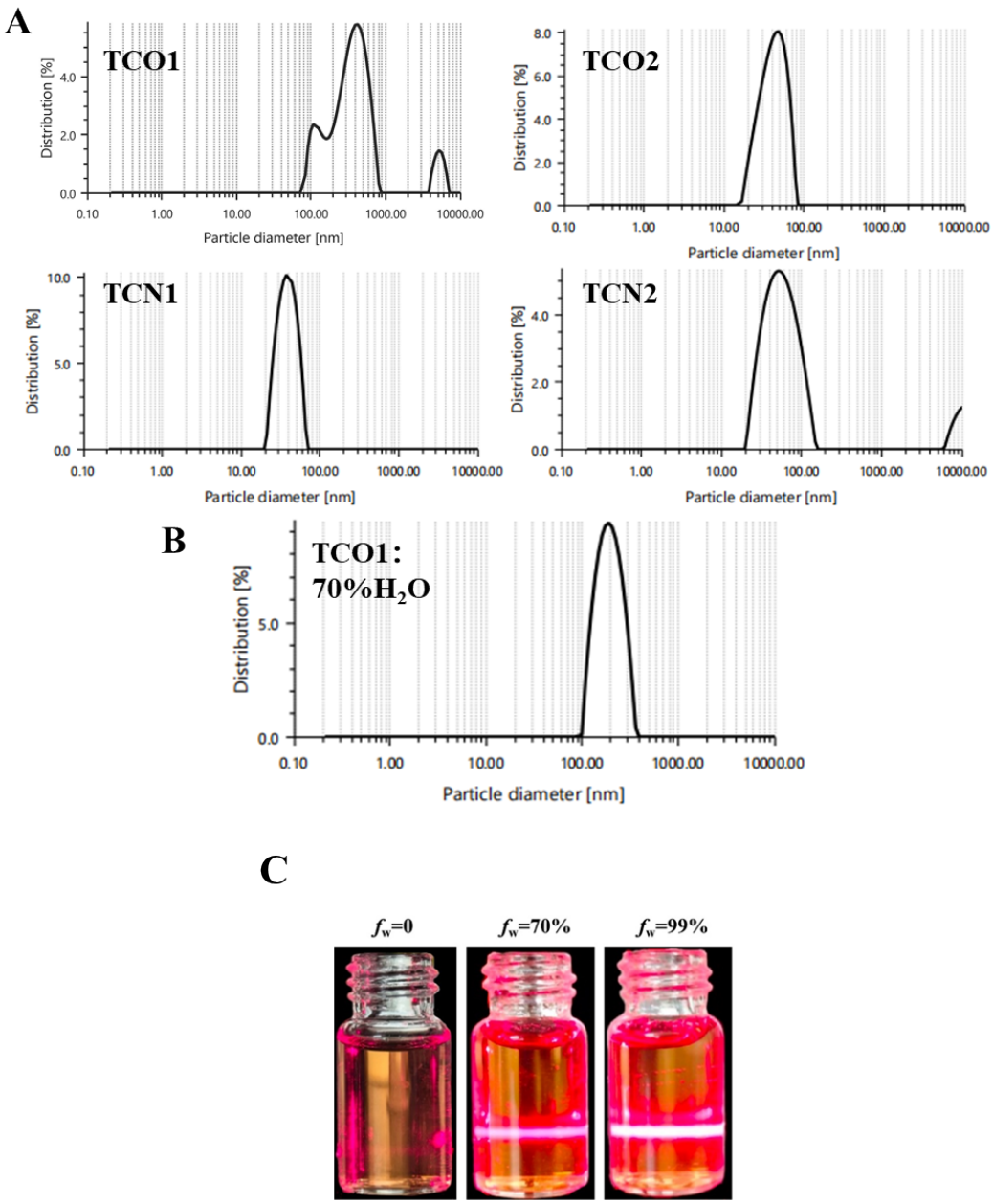

Fig. S3 (A) Particle diameter detection of compounds **TCO1**, **TCO2**, **TCN1** and **TCN2** in water. (B) Particle diameter detection of compounds **TCO1** in the 70% water content. (C) Tyndall effect diagram of compound **TCO1** in ethanol, 70% water and 99% water, respectively.

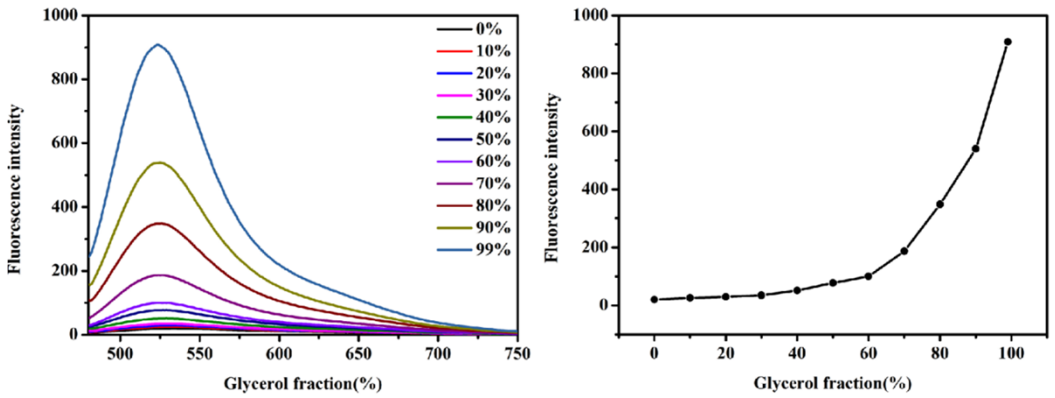

Fig. S4 Fluorescence emission spectra of compound **TCO1** in different glycerol ratios of methanol and glycerol mixtures.

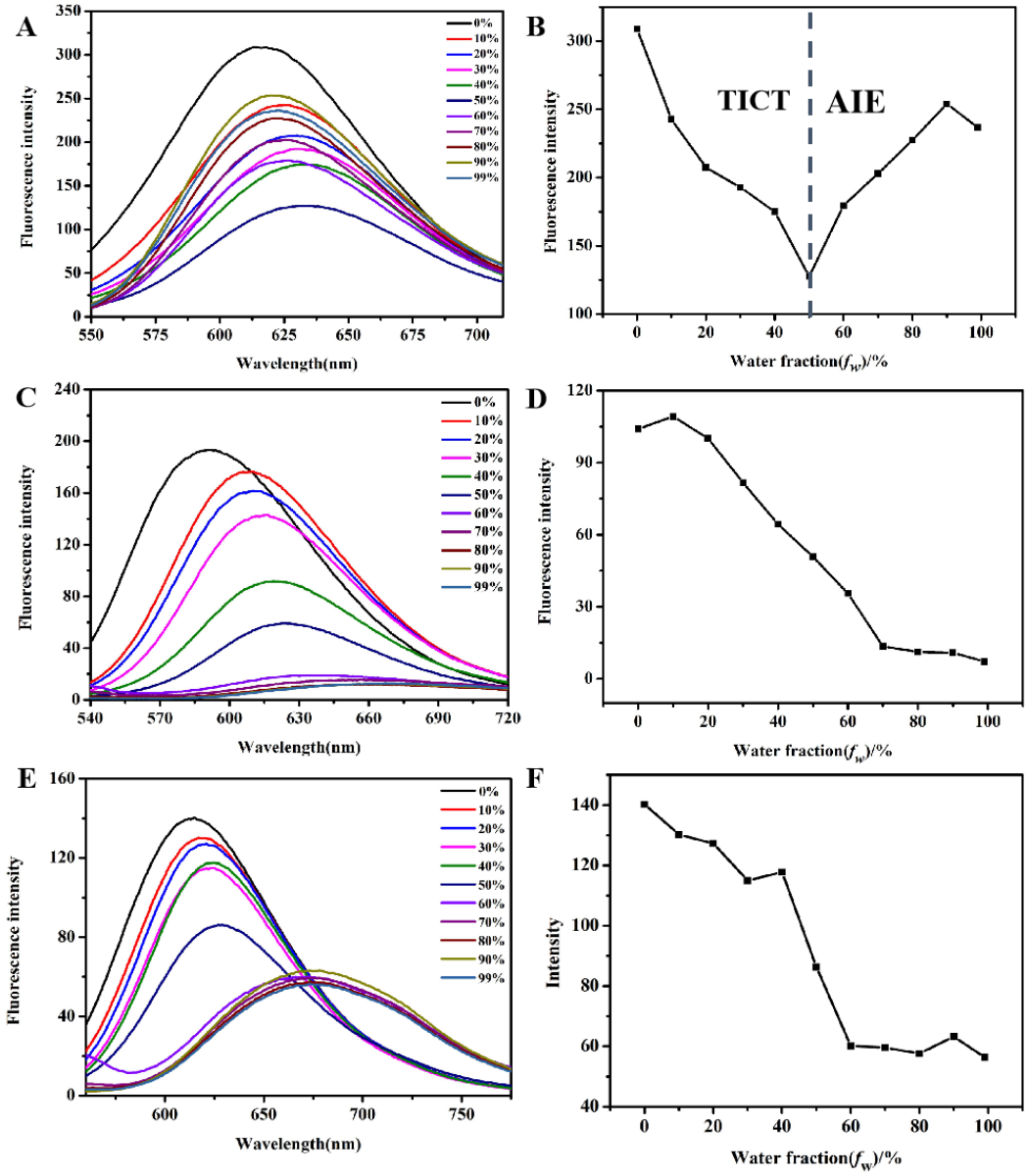

Fig. S5 Fluorescence emission spectra of compounds **TCO2**, **TCN1** and **TCN2** in ethanol/water at different water ratios.

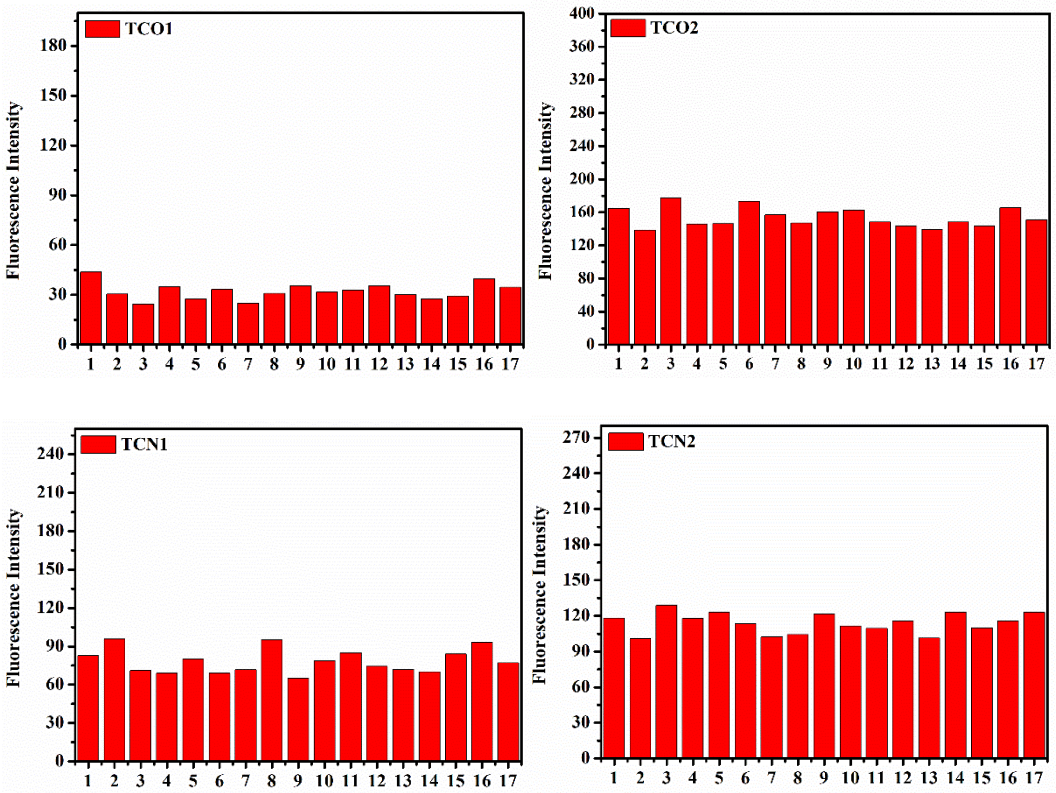

Fig. S6 Fluorescence intensity of compounds **TCO1**, **TCO2**, **TCN1** and **TCN2** in the presence of different analytes. 1. Blank, 2. Cys, 3. H_2O_2, 4. Hcy, 5. KCl, 6. $Na_2S_2O_4$, 7. Na_2SO_4, 8. NaBr, 9. NaF, 10. NaHS, 11. L-phenylalanine, 12. L-lysine, 13. L-tyrosine, 14. L-leucine, 15. L-proline, 16. Glucose, 17. L-tryptophan.

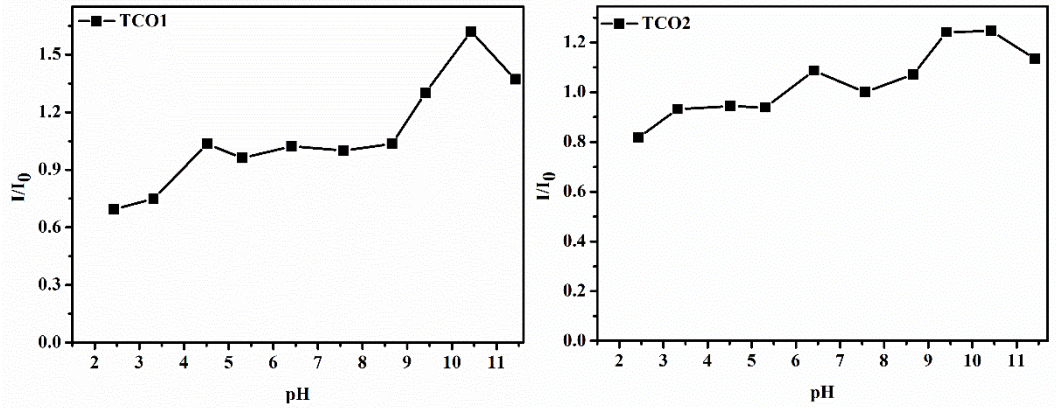

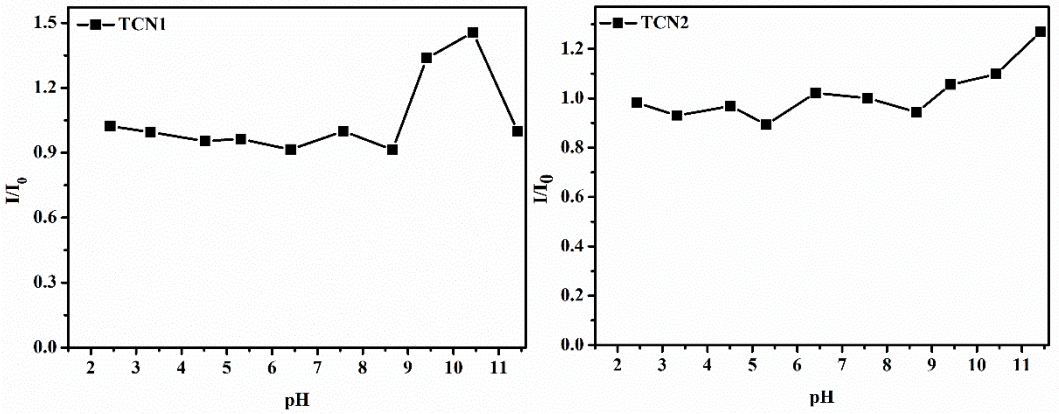

Fig. S7 Fluorescence intensity ratios I/I_0 of compounds **TCO1**, **TCO2**, **TCN1** and **TCN2** in different pH environments. I represents the fluorescence intensity of compounds at different pH solution, I_0 represents the fluoresce intensity of compounds at pH=7.57.

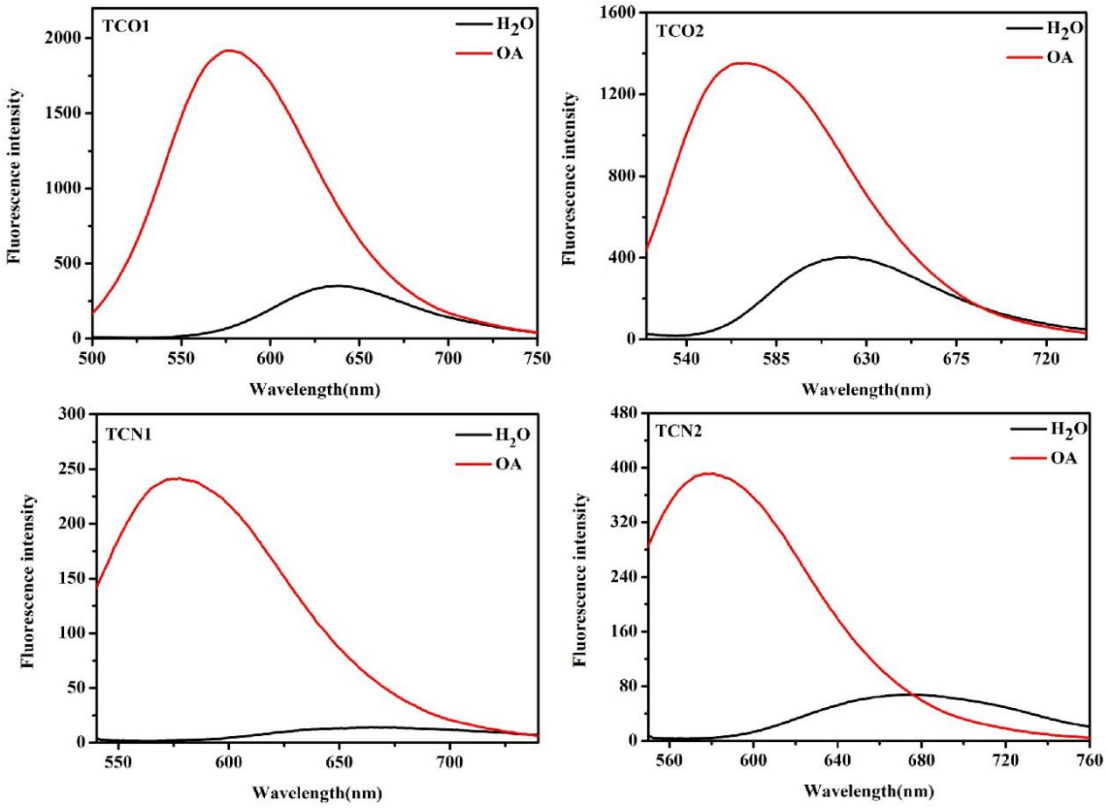

Fig. S8 Fluorescence intensity of compounds **TCO1**, **TCO2**, **TCN1** and **TCN2** in solvent with water and oleic acid (OA), respectively.

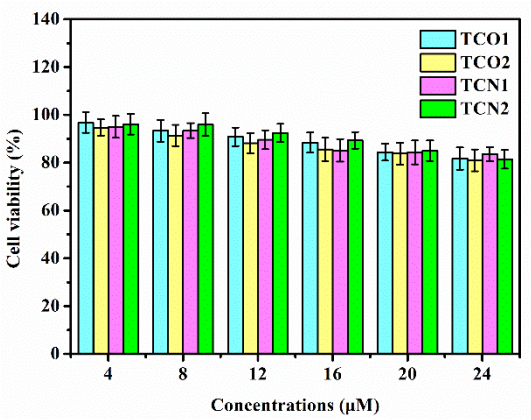

Fig. S9 Cytotoxicity experiments of compounds **TCO1**, **TCO2**, **TCN1** and **TCN2**.

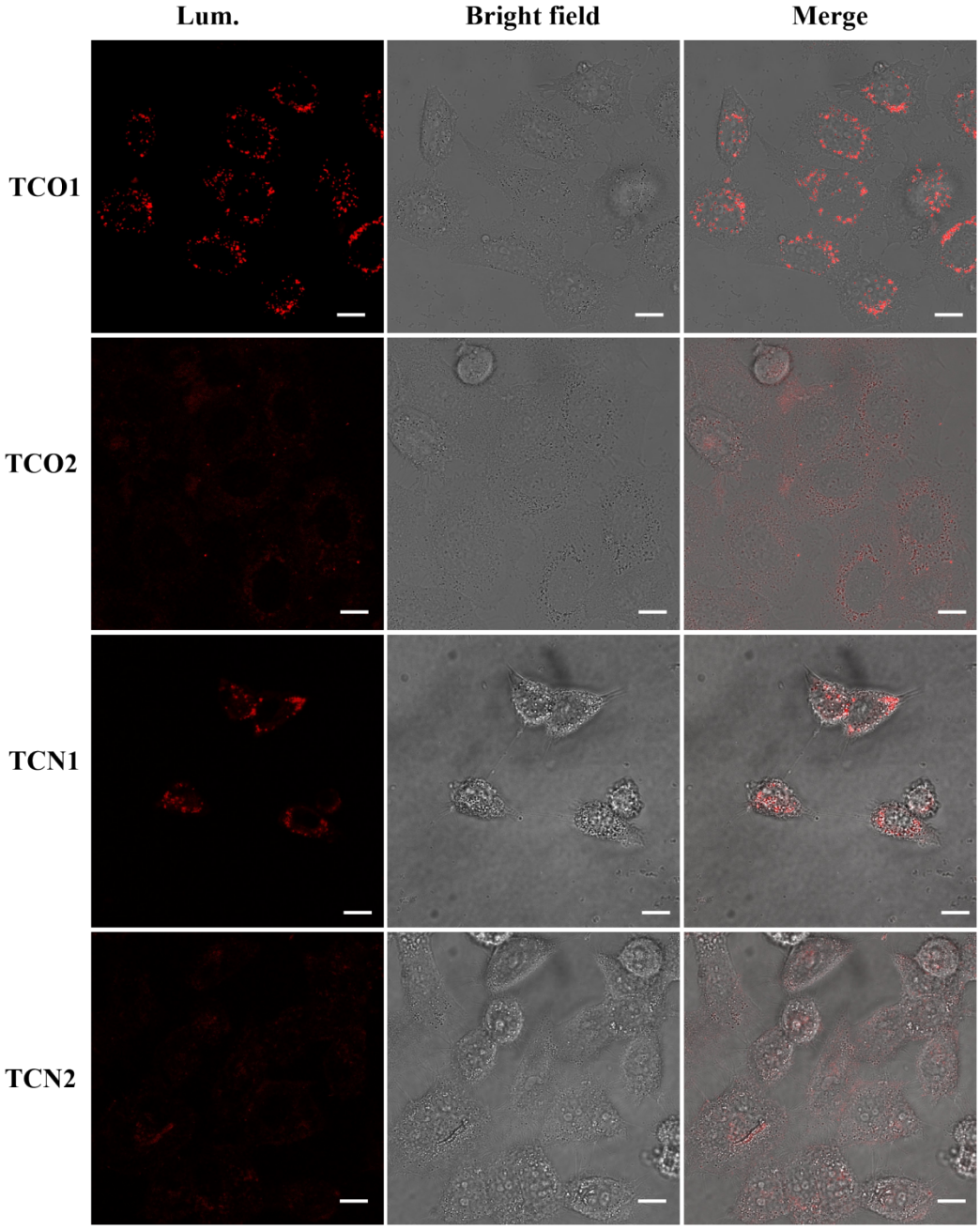

Fig. S10 Cell imaging of compounds **TCO1**, **TCO2**, **TCN1** and **TCN2** in live HepG2 cells respectively. Scale bar: 10 μm. For **TCO1**, λ_{ex}=442 nm, λ_{em}= 550-620 nm. For **TCO2**, λ_{ex}=442 nm, λ_{em}= 550-620 nm. For **TCN1**, λ_{ex}=514 nm, λ_{em}= 560-650 nm. For **TCN2**, λ_{ex}=514 nm, λ_{em}= 560-650 nm.

Table R1 Comparison of properties of **TCO1** and other lipid droplet fluorescence probes

Probe	Emission maxima (nm)	AIE feature	Wash-free	Application	Ref
2	517	√	/	cell imaging	[1]
LCH	627	/	/	cell imaging	[2]
CA-LD	640	/	/	cell imaging and zebrafish imaging	[3]
BLD2	725	/	/	cell imaging	[4]
TQE	584	√	/	cell imaging	[5]
MFGNI-1	511	/	/	cell imaging	[6]
DCI-Cou-polar	766	/	/	cell imaging and tissue imaging	[7]
P(Cou-PEG-LD)	475	/	/	cell imaging and zebrafish imaging	[8]
PPF-1	590	/	/	cell imaging	[9]
BTDA-RSS	520	/	/	cell imaging and tissue imaging	[10]
TPA-DT-DNH	530	/	/	cell imaging and zebrafish imaging	[11]
CH_3O-Ph_2N-S-TTz-Py	626	/	/	cell imaging, tissue imaging and C. elegans imaging	[12]
L	540	√	/	cell imaging	[13]
CIV	425	/	/	cell imaging	[14]

SSR-LDs	650	/	/	cell imaging, zebrafish imaging and mice imaging	[15]
TCO1					

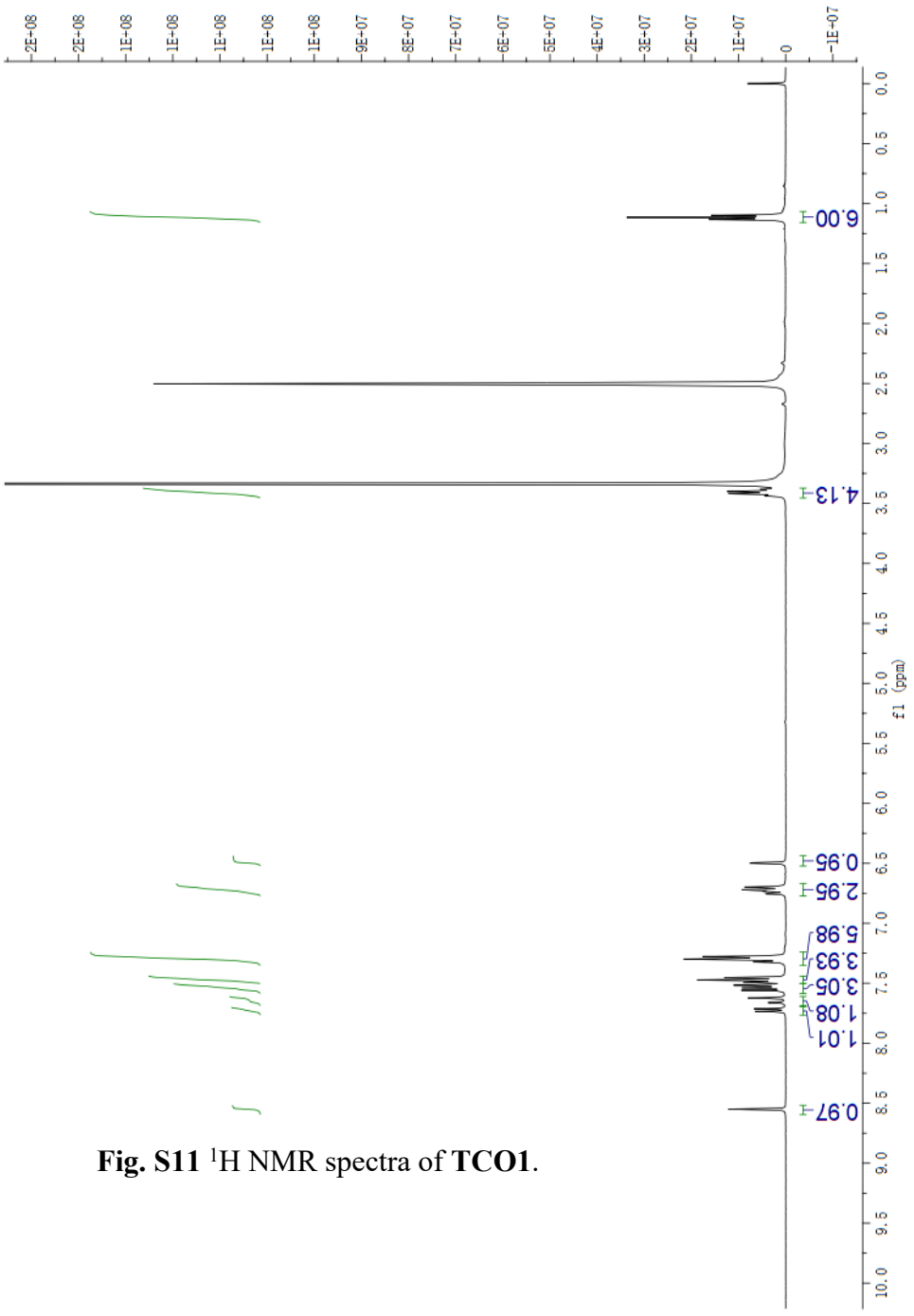

Fig. S11 ^{1}H NMR spectra of **TCO1**.

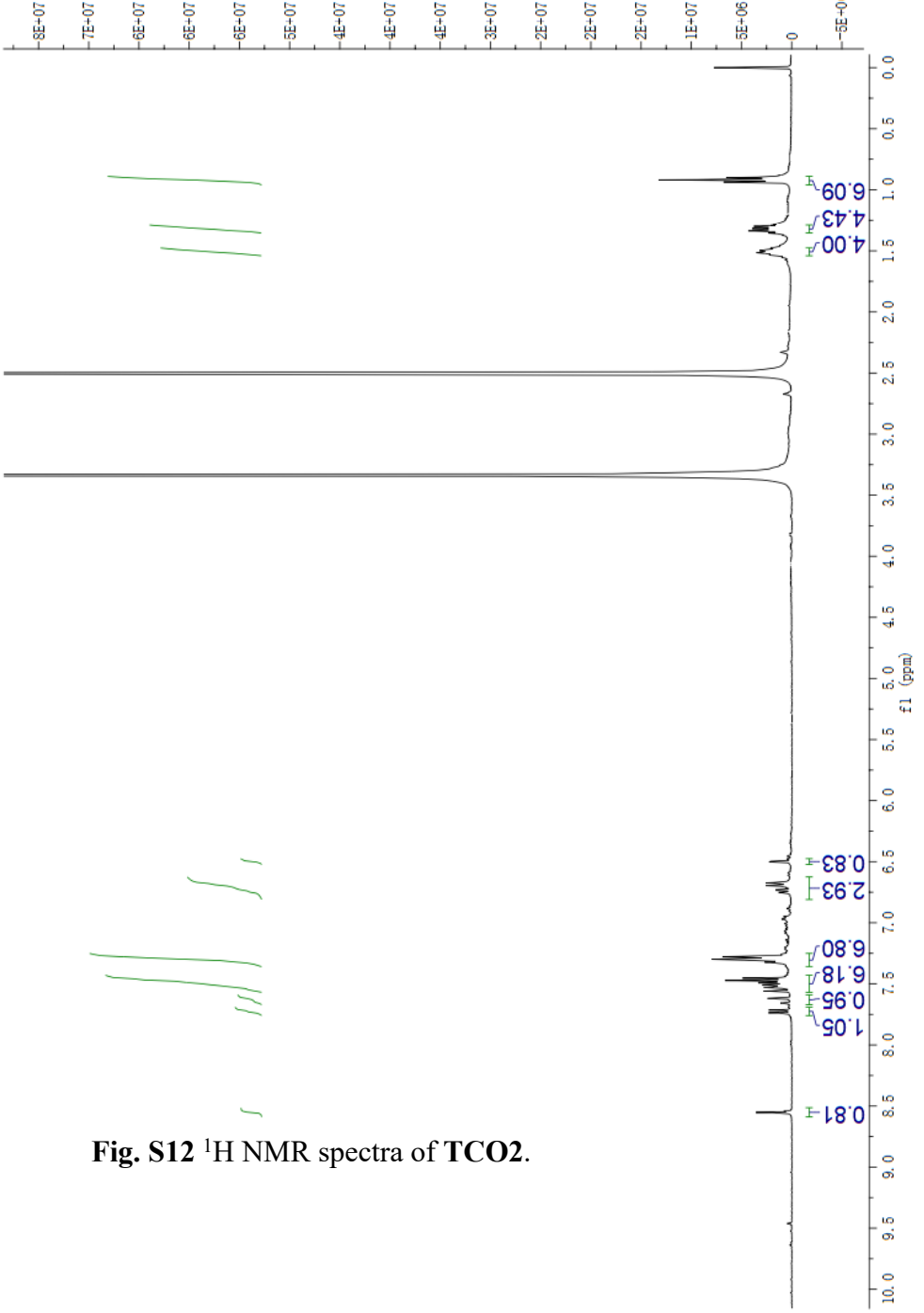

Fig. S12 ^{1}H NMR spectra of **TCO2**.

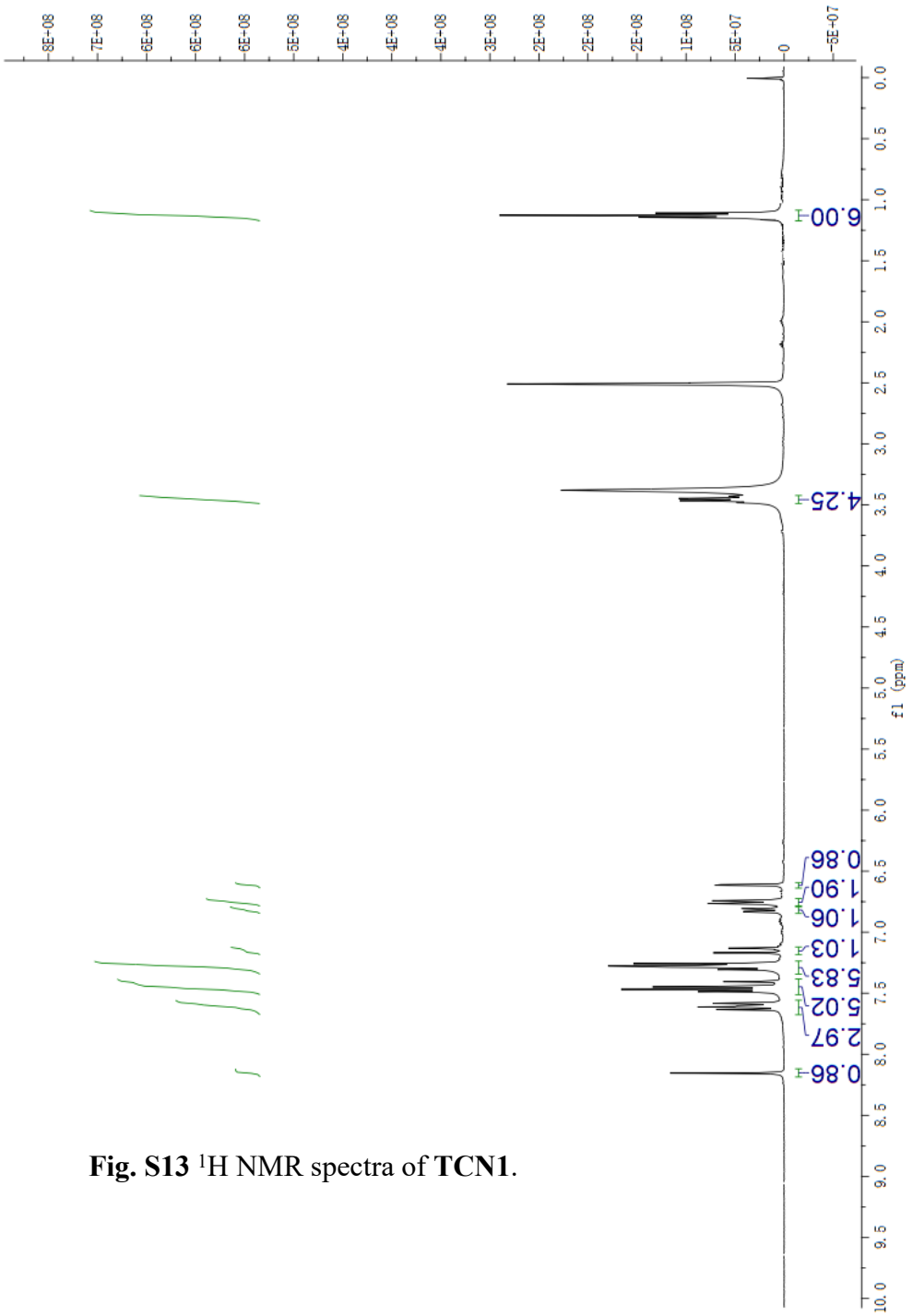

Fig. S13 ^{1}H NMR spectra of **TCN1**.

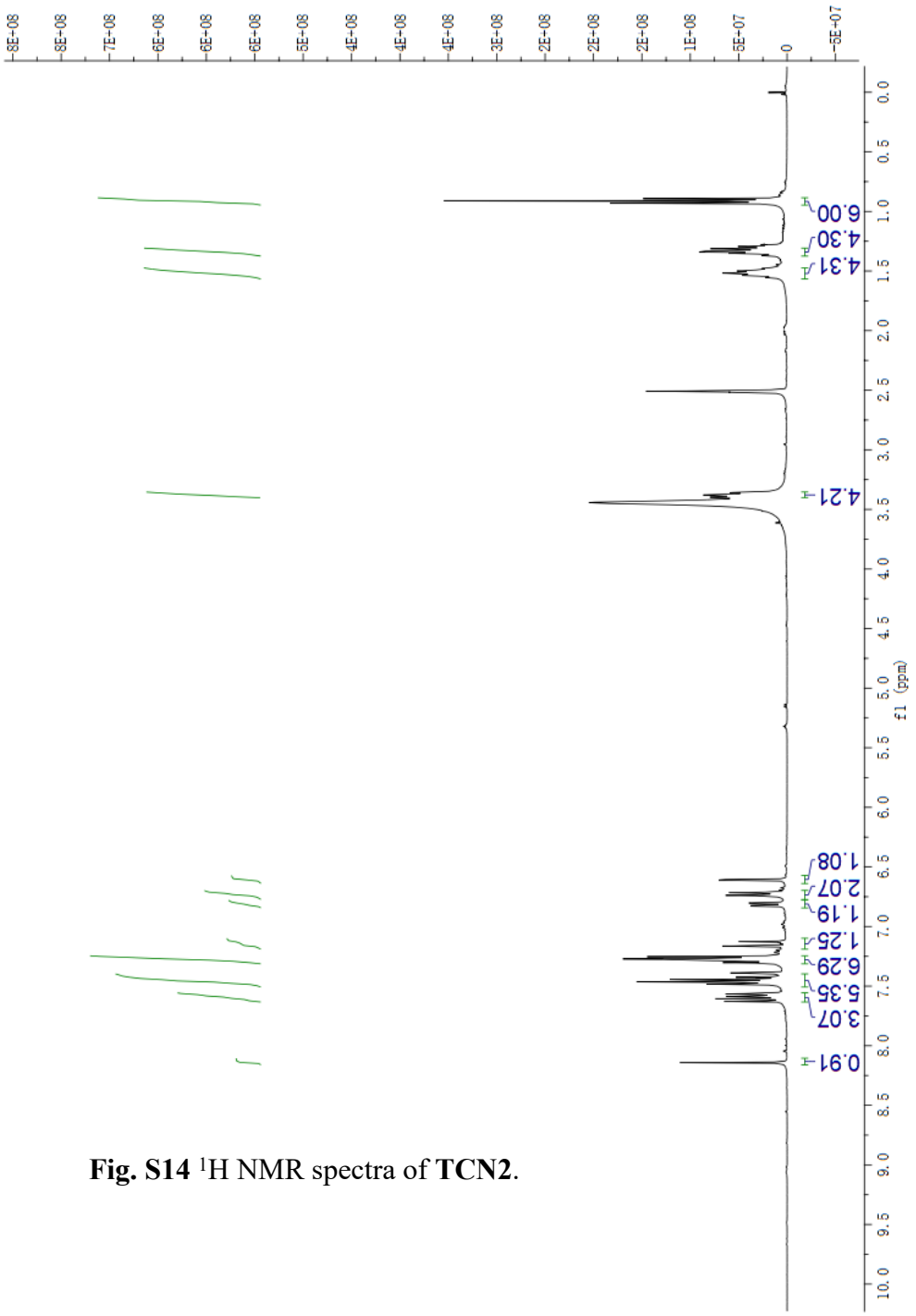

Fig. S14 ^{1}H NMR spectra of **TCN2**.

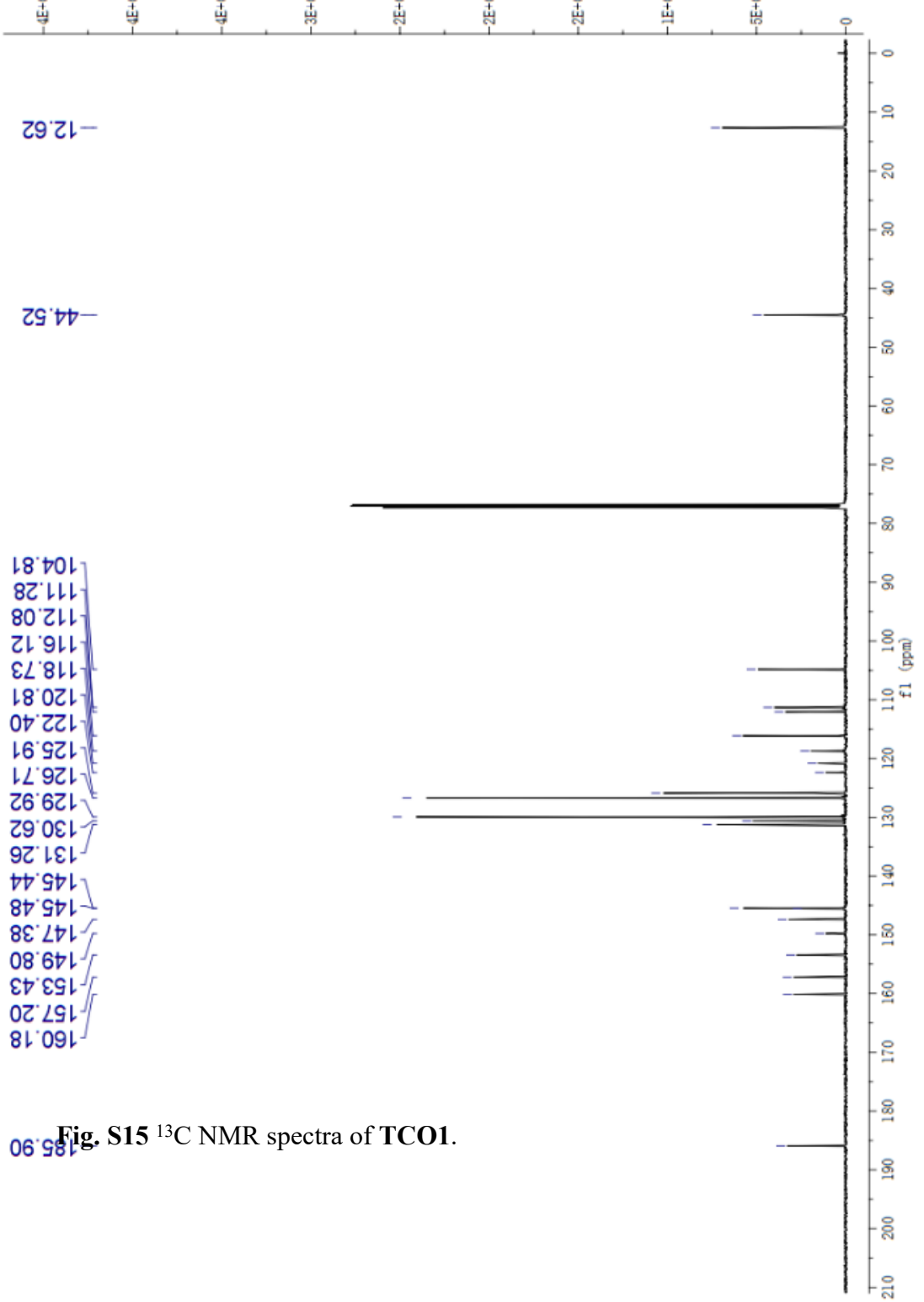

Fig. S15 ^{13}C NMR spectra of **TCO1**.

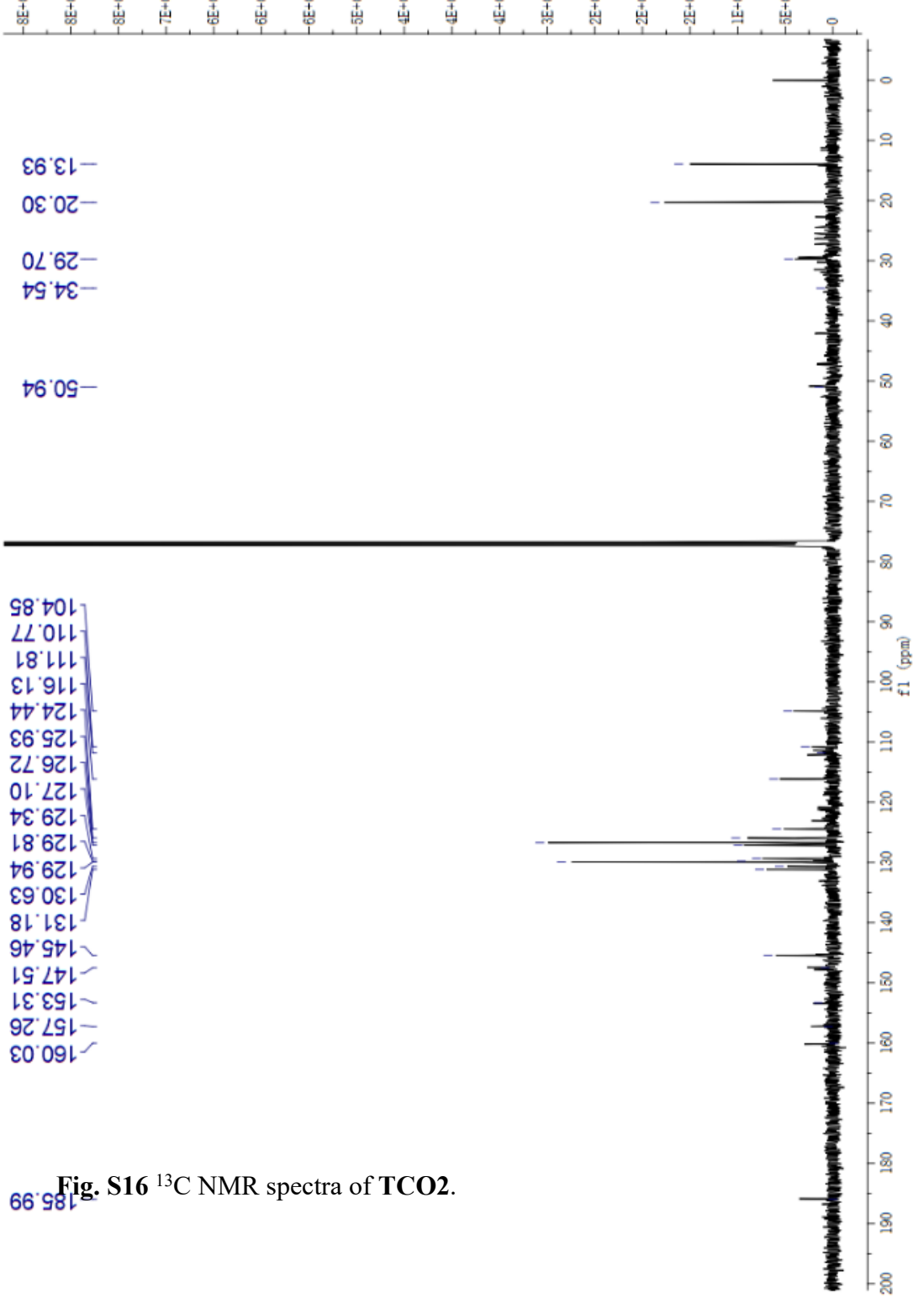

Fig. S16 ^{13}C NMR spectra of **TCO2**.

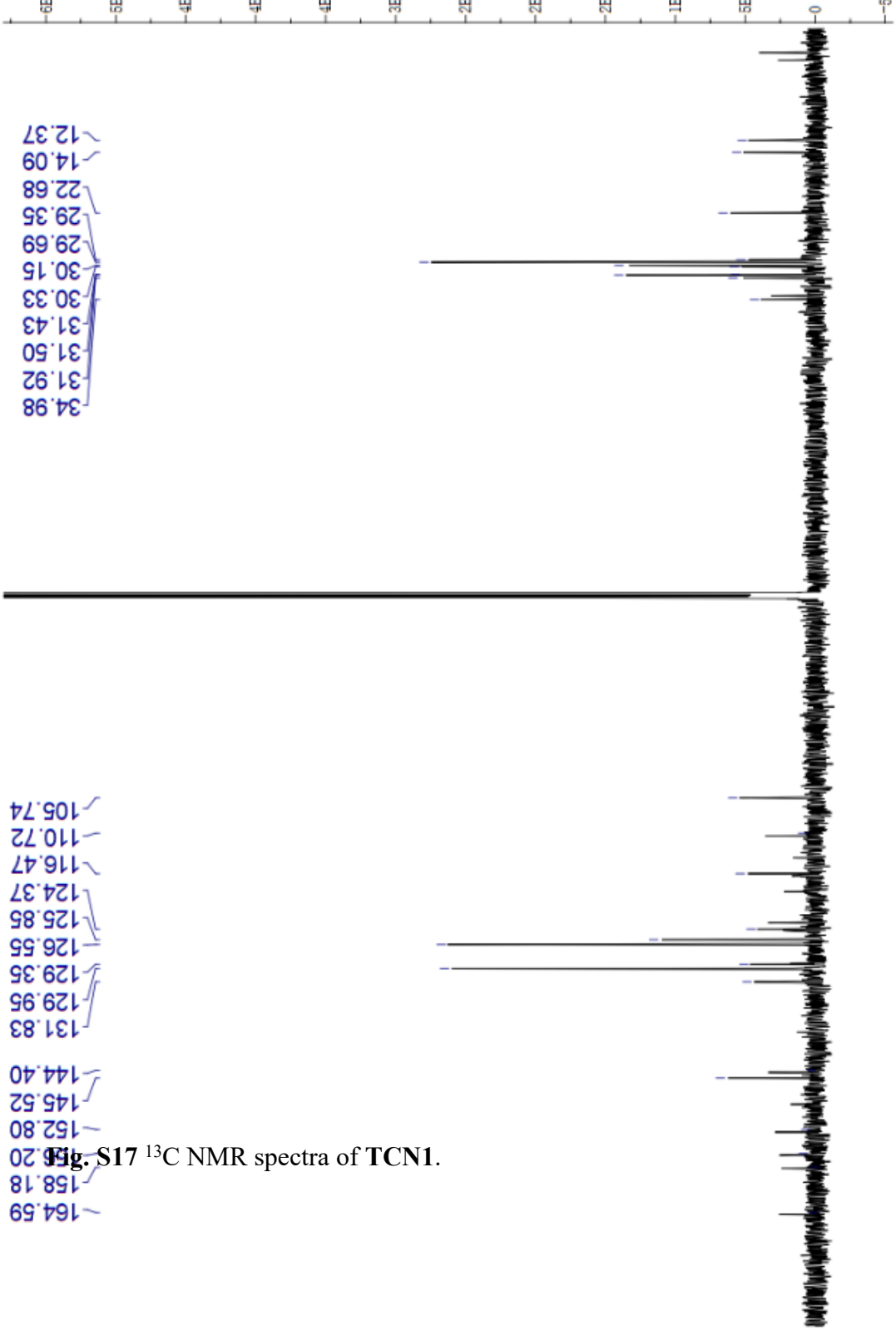

Fig. S17 ^{13}C NMR spectra of **TCN1**.

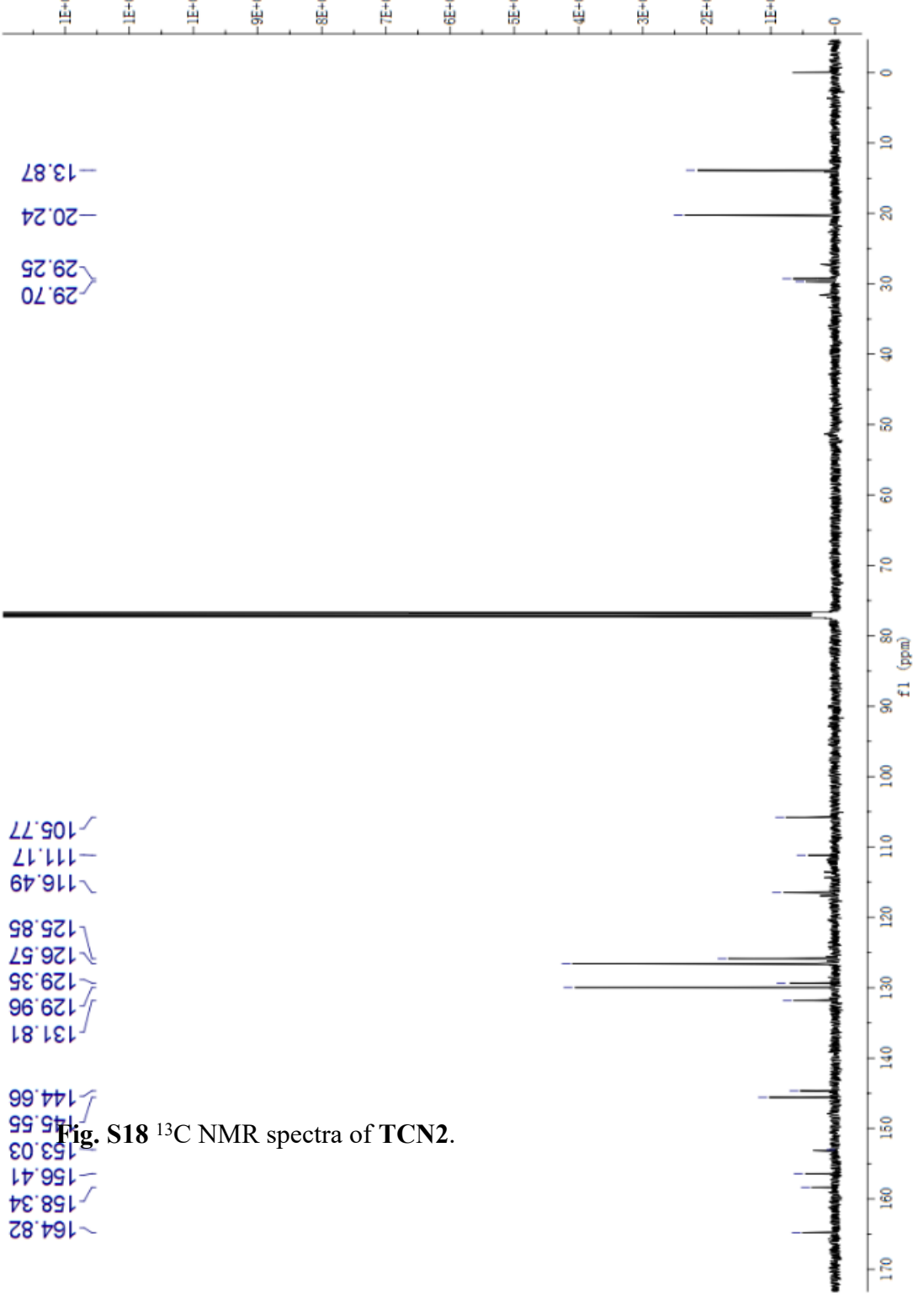

Fig. S18 ^{13}C NMR spectra of **TCN2**.

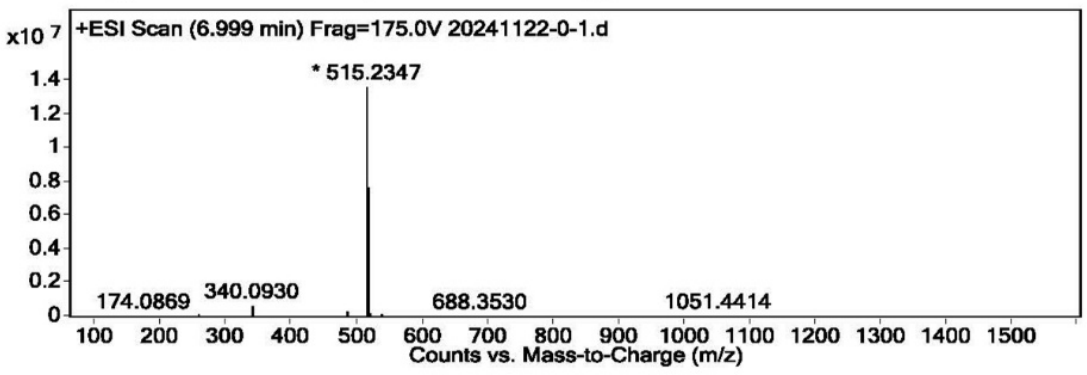

Fig. S19 HRMS spectra of **TCO1**.

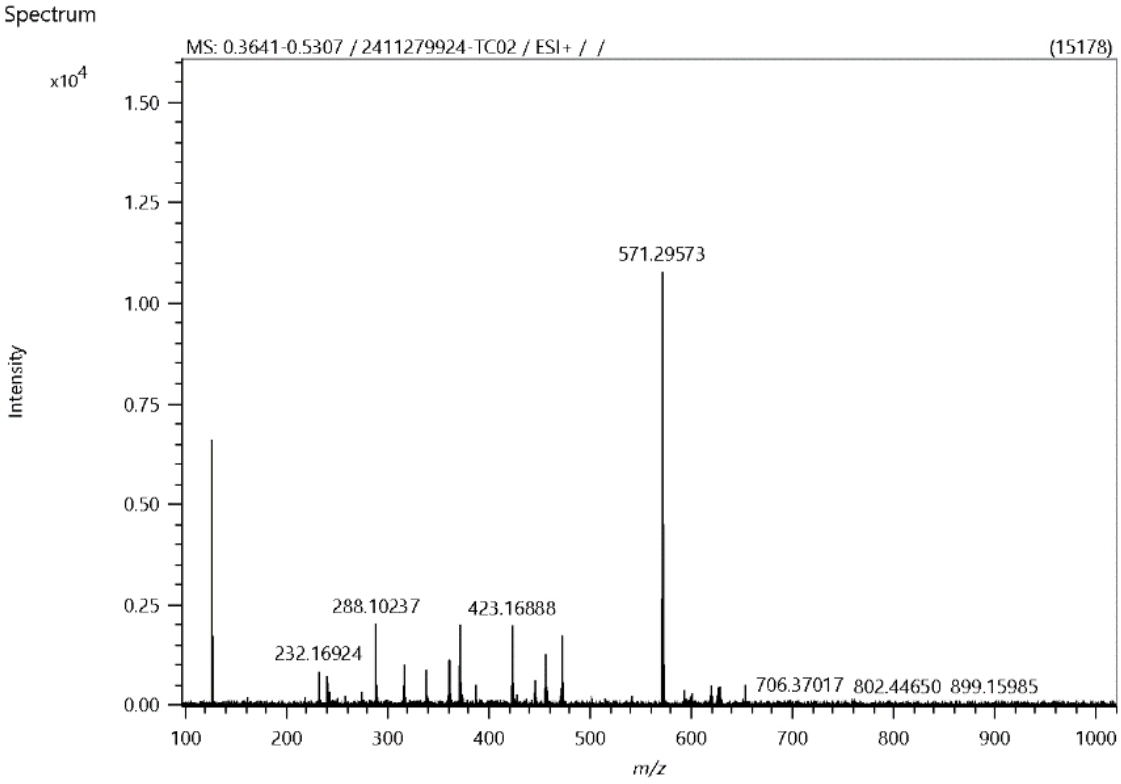

Fig. S20 HRMS spectra of **TCO2**.

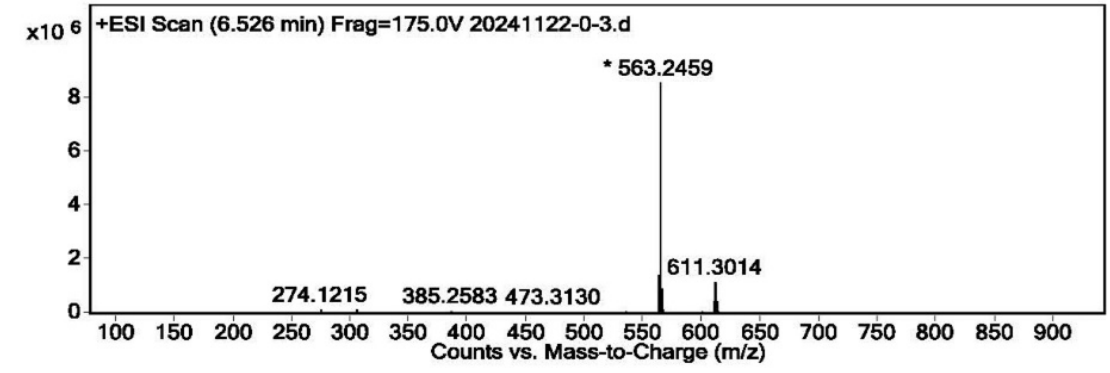

Fig. S21 HRMS spectra of **TCN1**.

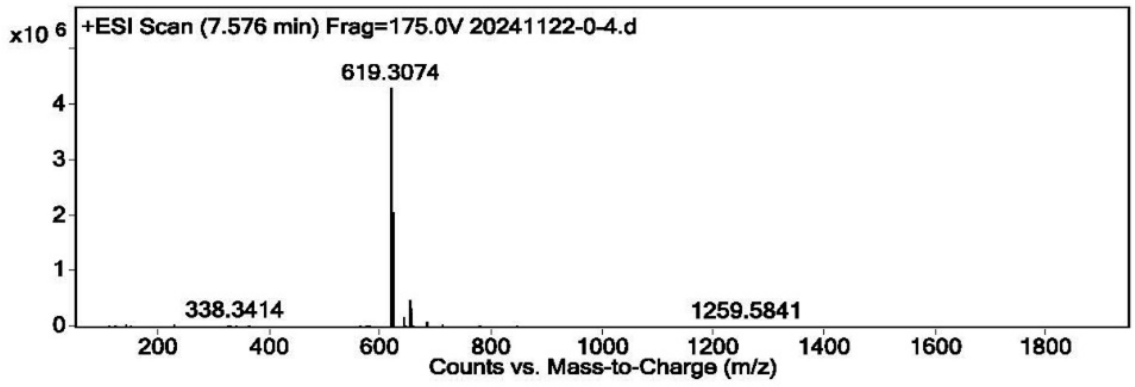

Fig. S22 HRMS spectra of **TCN2**.

Reference

[1] P. J. Choi, Y. Tatenaka, K. Noguchi, M. Ishiyama, W. Denny and J. Jose, ChemBioChem, 2024, 25, 415.

[2] Y. Y. Cui, Y. Y. Meng, Y. Hu, Y. Q. Chen, Y. X. Yang, M. Fang, C. Li and W. J. Zhu, J. Chin. Chem. Soc., 2023, 1, 68-75.

[3] H. Zheng, G. F. Li, L. D. Zhang, M. G. Fan and W. Y. Lin, New J. Chem., 2024, 38, 16710-16717.

[4] O. H. Javier, F. M. Fernanda and J. S. Arturo, Tetrahedron, 2024, 1, 134354.

[5] B. Zhang, Y. R. Zhang, C. J. Wang and J. Y. Jin, J. Fluoresc., 2023, 15.

[6] X. W. Li, J. Q. Bian, M. Y. Fu, Y. Zhang, H. M. Liu and B. X. Gao, Anal. Methods, 2022, 12, 1279-1284.

[7] S. Zhu, L. X. Dai, X. L. Zhong and W. Y. Lin, Anal. Methods, 2024, 18, 2850-2856.

[8] W. L. Cui, M. H. Wang, Y. H. Yang, J. B. Qu, H. T. Zhang, X. Z. Zhu and J. Y. Wang, New J. Chem., 2022, 34, 16539-16546.

[9] S. F. Ma, L. Y. Ma, P. Y. Wan, L. Y. Li, Z. X. Huang, Q. Yu, B. Y. Zhang, L. X. Guo, L. L. Yan, L. H. Li, H. J. Wang, B. Wang, H. P. Diao, W. Liu and C. W. Zhang, Sens. Actuators B Chem., 2024, 1, 136441.

[10] Y. W. Zhang, N. Zhang, S. H. Wang, Q. Zan, X. D. Wang, Q. Q. Yang, X. Yu, C. Dong and L. Fan, Analyst, 2022, 8, 1695-1701.

[11] Y. X. Wang, W. L. Yan, Y. Liu, H. Z. Du, G. M. Zhang, C. H. Zhang, S. M. Shuang, C. Dong, J. Mol. Struct., 2025, 3, 139994.

[12] Q. Wang, D. M. Li, Z. Zhang, L. Y. Shen, H. Xu, Z. Y. Wang, C. Radshaw and Q. L. Zhang,

Spectrochim. Acta. A Mol. Biomol. Spectrosc., 2025, 5, 125694.

[13] R. Valand, N. Pandye, D. S. Bandaru and D. A. Sivaiah. ChemistrySelect, 2023, 43, 3697.

[14] H. Y. Chen, J. Z. Zhao, J. Z. Lin, B. L. Dong, H. Li, B. Geng and M. Yan, RSC Adv., 2021, 11, 8250.

[15] Y. H. Tang, S. Song, J. J. Peng, Q. Zhang and W. Y. Lin, J. Mater. Chem. B, 2022, 10 6974.